A monatomic system with a liquid-liquid critical point and two distinct glassy states

Limei Xu,[1,2,a)] Sergey V. Buldyrev,[3] Nicolas Giovambattista,[4] C. Austen Angell,[5] and H. Eugene Stanley[1]
[1]*Center for Polymer Studies and Department of Physics, Boston University, Boston, Massachusetts 02215, USA*
[2]*World Premier International (WPI) Research Center, Advanced Institute for Materials Research, Tohoku University, Sendai 980–8577, Japan*
[3]*Department of Physics, Yeshiva University, 500 West 185th Street, New York, New York 10033, USA*
[4]*Department of Physics, Brooklyn College of City University of New York, Brooklyn, New York 11210, USA*
[5]*Department of Chemistry and Biochemistry, Arizona State University, P.O. Box 871604, Tempe, Arizona 85287, USA*

(Received 18 August 2008; accepted 17 November 2008; published online 6 February 2009)

We study the glass transition (GT) in a model system that exhibits the presence of more than one liquid or glassy state ("polyamorphism") using molecular dynamics simulations. We study the Jagla model [E. A. Jagla, J. Chem. Phys. **111**, 8980 (1999)], a two-scale spherically symmetric ramp potential with both attractive and repulsive interactions. The Jagla model is particularly interesting since, depending on its parametrization, it predicts two phases ("polyamorphism") not only in the glassy state but also in equilibrium as a liquid-liquid phase transition (LLPT). The Jagla model may also be useful in understanding a recent observation of polyamorphism in metallic glasses containing cerium. We use a parametrization for which crystallization can be avoided and the GT and LLPT are clearly separated, providing a unique opportunity to study the effects of the LLPT on the GT. We follow the experimental protocol employed in the classical differential scanning calorimetry experiments used to characterize the GT, cooling and heating the system through the GT and calculating the constant-pressure specific heat C_P and the thermal expansion coefficient α_P. At pressures below and well above the LLPT, the same basic GT phenomenology of metallic glasses is observed, i.e., a single peak in C_P (typical of ergodicity restoration) occurs upon heating across the GT. At pressures above the LLPT, a second peak in C_P develops at higher temperature above the GT. This second peak in C_P arises from the presence of a Widom line T_W defined as the locus of maximum correlation length in the one-phase region above the liquid-liquid critical point (LLCP). The behavior of α_P is different across the GT and Widom line. Near the GT temperature T_g, α_P displays a small peak upon heating, which makes a negligible contribution to the C_P peak. On the other hand, near T_W, α_P displays a much larger peak, which makes a substantial contribution to the C_P peak at higher temperature. We find that T_g is almost independent of pressure for each of the two coexisting liquids, but shows an apparent discontinuity upon crossing the LLPT line, to a lower value for the higher-entropy phase. We compare the entropies of both phases, and the corresponding temperature dependencies, with those of the crystal phase. We also study the dependence of the GT on heating rate and find that for pressures below the LLCP, slow heating results in crystallization, as occurs in laboratory experiments. Regarding the thermal expansion properties of the Jagla model, we study the interplay of the density minimum recently observed in confined water and the GT. [DOI: 10.1063/1.3043665]

I. INTRODUCTION

The existence of two or more distinct glasses in a single-component substance was first observed in water.[1] In 1935, Oliver and Burton[2] described amorphous solid water (ASW) as the product of low-temperature vapor deposition. In 1974, Venkatesh *et al.*[3] described a second form of ASW produced by vapor deposition that was 14% denser than ASW. The possibility that amorphous systems could exist in more than one distinct state ("polyamorphism") became widely appreciated a decade later when Mishima *et al.*[4] studied the amorphization of ice upon pressurization and discovered that water could exist as a high-density amorphous (HDA) form, which if recovered at ambient pressure and then annealed,[5] transformed into a material apparently the same in structure as the ASW found by Oliver and Burton. Subsequently, a number of instances of such laboratory transformations have been reported[6] including elemental,[7,8] molecular,[9] ionic,[10] and covalent[11] systems. Most recently, a metallic glass case, based on cerium,[10] has been added to the list. These are all

a)Electronic mail: limei.xu@wpi-aimr.tohoku.ac.jp.

examples of the phenomenon of polyamorphism, a topic that is now receiving considerable attention. Three reviews have recently appeared.[12–14]

Most of the experimental studies on polyamorphism involve transitions from an initial liquid state to either a second metastable liquid or to a glass. Polyamorphism in equilibrium, i.e., a liquid-liquid phase transition (LLPT),[15] has been recently studied experimentally for bulk water,[16] for bulk phosphorus,[7] for quasi-two-dimensional confined water,[17,18] and for quasi-one-dimensional confined water,[19–22] as well as for the thin layer of water surrounding biomolecules such as lysozyme, DNA, and RNA.[20,23]

Although some simulation studies of polyamorphic phenomena have also found LLPTs to be a metastable state phenomenon,[15] there is a class of cases in which the LLPT is found at much higher temperatures and under thermodynamically stable conditions. These are systems composed of particles interacting with a spherically symmetrical pair potential characterized by a hard core with a soft-core repulsion and followed by an attractive part at larger separations. These are known as "soft-core" pair potentials.[24] It has been suggested that such potentials provide a generic mechanism for LLPT,[25] and has interested experimentalists to seek examples among the liquid metals.[10] Stell and Hemmer[24] identified cesium and cerium as candidate systems, and indeed irreversible density changes under high pressure in glassy metals containing a large mole fraction of Ce have subsequently been reported.[10]

There is evidence from several sources[26–29] that the two liquid phases involved in a LLPT have rather different properties. Not only does the lower temperature phase have a considerably reduced fluidity, as expected from its lower entropy, but its temperature dependence is more Arrhenius (less "fragile").[19,26] It can be challenging to establish such properties unambiguously because of the propensity of the low-entropy liquid to crystallize. It is therefore of interest to find a model system in which both liquid phases can be studied under stable as well as metastable conditions, and in which the glass transitions (GT) can be observed independently.

One such model system was recently identified, the Jagla model[30] [Fig. 1(a)]. This model was previously investigated[26,31–33] and found to have a LLPT. In the present parametrization of Fig. 1(a), the LLPT line extends into the *equilibrium* liquid phase, ending in a liquid-liquid critical point (LLCP) as shown in the schematic phase diagram of Fig. 1(b). The ergodic behavior of the Jagla model was examined in some detail in Ref. 26, but its glassy states and features, such as the changes of isobaric specific heat C_P at the GT, were left uncharacterized.

Here we address the low-temperature properties of the two liquid phases directly and observe the relation of their thermodynamic behavior through the GT to the ergodic behavior of the system in the vicinity of the LLCP. The choice of model parameters needed to place the LLCP of our system within the stable liquid region excludes direct relation to the polyamorphic behavior of cerium-based glasses. However, the two systems are close enough, phenomenologically, that we should be able to predict the relations between high-density and low-density metallic liquid phases that might be found in future studies of cerium-rich bulk metallic glass-formers.

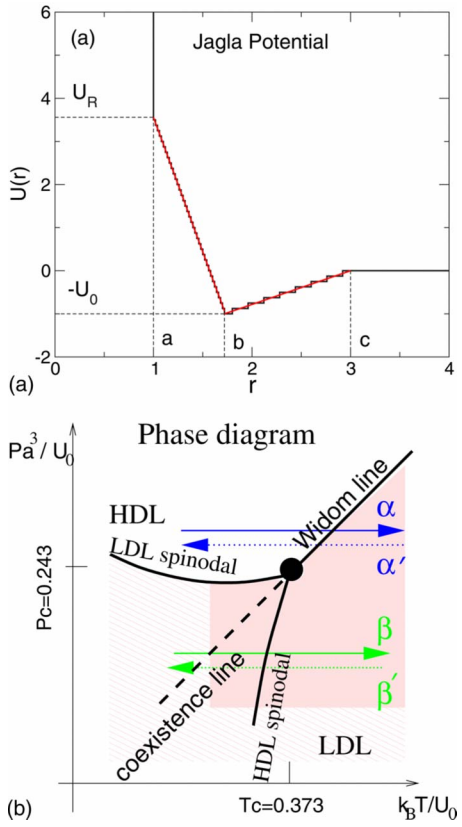

FIG. 1. (Color online) The spherically symmetric "two-scale" Jagla ramp potential and a sketch of its phase diagram. (a) The two length scales of the Jagla potential are the hard-core diameter $r=a$ and the soft-core diameter $r=b$. Here we treat the case with $U_R=3.56U_0$, $b=1.72a$, and a long range cutoff $c=3a$. The discretized version of the potential studied here (black bold line) is shown along with the original potential (red). We use a discretization step, $\Delta U=U_0/8$. (b) Sketch of the Jagla potential P-T phase diagram (Ref. 26). The LDL and HDL phases are separated by a first order transition line (dashed line), terminating at a critical point at $P_c=0.243$ and $T_c=0.373$. The Widom line T_W indicates the locus of maxima in the correlation length that occurs at $T>T_c$ and $P>P_c$. Studies in this work are along four different kinds of paths: (i) for $P>P_c$, path α (heating) and path α' (cooling), and (ii) for $P<P_c$, path β (heating) and path β' (cooling).

The existence of a single-component, monatomic, system with two distinct glassforming liquid phases provides a rare opportunity for study of fundamental aspects of glass formation. Kauzmann first provided the evidence that glassformers in general suffer from an entropy problem. With a few exceptions, provided by the inorganic network cases, glassformers show variations with temperature of their total entropies which would cause them to violate statistical mechanical fundamentals by achieving negative entropies, unless some dramatic change in their properties occurs at temperatures not far below those of their T_g values. Closer to their T_g values: the liquid entropies would fall below their crystal values, which is also not easily accepted. The temperature where the extrapolated liquid entropy would cross the crystal value has become known as the Kauzmann temperature, and it is believed that some change must occur in the equilibrium properties of the supercooled liquid to prevent such a crossing. A number of theories of glassformer

thermodynamics are predicated on the notion that the Kauzmann temperature is the "theoretical starting point" for the liquid state. The possibility that a single system could have two such starting points, depending on which of the two liquid phases is being examined, is an important question to investigate, as is the relationship between the excess entropies of the two liquid phases at their respective T_g values.

In the present work we will study, using the same approach adopted in experiments, the equilibrium properties of the two liquid phases of the Jagla model, and the freezing and unfreezing of equilibrium at the GT. We follow the experimental protocol employed in differential scanning calorimetry (DSC) experiments used to characterize the GT. We cool and heat the system through the GT, and calculate the constant-pressure specific heat C_P and thermal expansion coefficient α_P at different pressures, above and below the LLCP [Fig. 1(b)]. DSC experiments show that C_P exhibits hysteretic behavior, generating peaks on heating and "smooth down steps" on cooling, in any temperature range in which a GT occurs.[14,16,34–42] The GT is also associated with a sharp change of α_P, thus providing an accurate experimental method of studying the GT at high pressure where other traditional methods such as DSC may be difficult to perform.[43] These phenomena are well understood from models incorporating non-Arrhenius, nonexponential, nonlinear features of viscous liquid phenomenology.[35,44] An LLPT, on the other hand, will produce a latent heat, while an LLCP and supercritical range will produce C_P and α_P spikes that will not be scan-rate dependent or scan-direction dependent (except very near the LLCP where fluctuations are very slow).

Another important question—especially relevant for liquids with density anomalies such as water, BeF_2, Si, and SiO_2—is how the anomalous thermal expansion behavior upon cooling below the temperature of maximum density T_{max} in the supercooled liquid changes to "normal" behavior in the glass state. Recent experiments on confined water[21] show the existence of a density minimum at $T_{min}=210$ K. These results are very important because they imply that there must be maxima in α_P, K_T, and C_P between T_{min} and T_{max}. These maxima may be associated with the Widom line emanating from the hypothesized LLCP. On the other hand, the experimentally observed density minimum may be associated with the dynamic arrest at the GT. The Jagla model is an ideal system to study this complex interplay because it possesses both a density minimum in the supercooled LDL state[45] and a GT. The main difference between phase diagrams of water and the Jagla model is that the latter has a *positive* slope of the LLPT coexistence line which is continued to the one-phase region by a *positively* sloped Widom line. The density anomaly in the Jagla model exists at pressures below the LLPT and therefore cannot be associated with the Widom line. Thus, studies of the Jagla model are useful for understanding of the general relations between the density anomaly and LLPT which may exist not only in water but also in other systems such as metallic glasses. Here we investigate how the GT phenomenology, as reflected by the behavior of C_P and α_P, is affected by the presence of a LLPT.

II. SIMULATION DETAILS

Our results are based on discrete molecular dynamics (MD) simulations[25,26,46,47] of a system composed of $N=1728$ particles interacting via the Jagla model,[30] which is characterized by not one but two characteristic length scales. This pair potential interaction, defined in Fig. 1(a), is characterized by a hard-core distance $r=a$ and a soft-core distance $r=b$. The attractive part of minimum energy $-U_0$ extends up to a distance $r=c$.

In what follows, all quantities reported are measured in reduced units. Distances and energies are in units of a and U_0, respectively. The simulation time t is measured in units of $a\sqrt{m/U_0}$, where m is the mass of the particle. The density of the system $\rho \equiv N/L^3$ is measured in units of a^{-3}, the pressure P is measured in units of U_0/a^3, the temperature T is measured in units of U_0/k_B, the specific heat C_p is measured in units of k_B, and the entropy S is measured in units of k_B.

In order to use the event-driven algorithm of discrete molecular dynamics,[48] we discretize the potential with a discretization step $\Delta U=U_0/8$, dividing the repulsive and attractive ramps, respectively, into 36 steps of width $0.02a$ and 8 steps of width $0.16a$, as shown in Fig. 1(a). The effects of discretization of the Jagla potential without an attractive ramp have been studied in Ref. 45 where it is shown that if the repulsive ramp is divided into more than 30 steps, the difference between the pressures given by the discretized and continuous potentials is less $0.01U_0/a^3$. Here we define $U_R=3.56U_0$ to be the value of the least squares linear fit to the discretized repulsive ramp at $r=a$. We find strong dependence of the critical pressure P_c and critical temperature T_c on U_R/U_0. Indeed, for $U_R/U_0=3.56$, $b/a=1.72$, and $c/a=3$ used in this work, we find $P_c=0.243U_0/a^3$ and $T_c=0.376U_0/k_B$, while for $U_R/U_0=3.05$, we find $P_c=-0.14U_0/a^3$ and $T_c=0.55U_0/k_B$. The values $P_c=0.17$ and $T_c=0.38$ obtained in Ref. 31 for $U_R/U_0=3.48$ are in agreement with our results.

We perform simulations at constant N, P, and T, where P is controlled by allowing the system box side length to change with time and T is controlled by rescaling the velocity of the particles. We perform cooling or heating simulations at a constant cooling/heating rate, $q \equiv \Delta T/\Delta t$. During these cooling/heating simulations, the reduced temperature T decreases/increases by ΔT over time Δt. We measure q in units of $q_0=\sqrt{U_0^3/ma^2k_B^2}$, e.g., $q_0=7.0\times10^{14}$ K/s if $a=0.27$ nm (corresponding to the first peak of the oxygen-oxygen pair correlation function in water), $U_0=4.75$ kJ/mol (in order to give the density maximum at maximum temperature of 277 K), and $m=36$ g/mol (since the mass of two water molecules corresponds to the mass of one Jagla particle within the hard-core distance[49]). Our lowest cooling rate ($10^{-6}q_0$) is one order of magnitude slower than the lowest cooling rate used in one MD simulation of water using the SPC/E model.[35]

III. RESULTS

A. Low-density glass and high-density glass

The observation of a LLPT in the Jagla model[30] suggests that two different glasses should exist at low temperature.

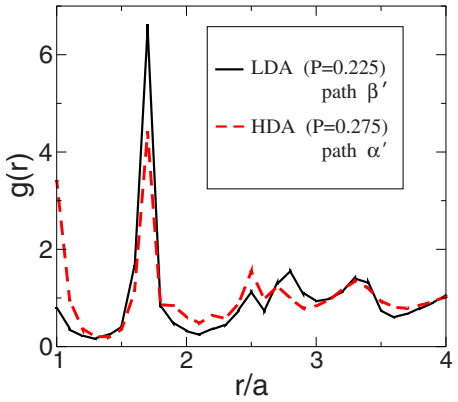

FIG. 2. (Color online) Illustration of the structural difference of the LDA solid and HDA solid by the RDF $g(r)$. The LDA solid is obtained upon cooling LDL along path β' ($P=0.225$). The HDA solid is obtained upon cooling HDL-like along path α' ($P=0.275$). Note that for HDA, particles shift from the soft-core distance ($r/a=1.72$) to the hard-core distance ($r/a=1.0$), so the peak at $r/a=1.72$ decreases while the peak at $r/a=1.0$ increases.

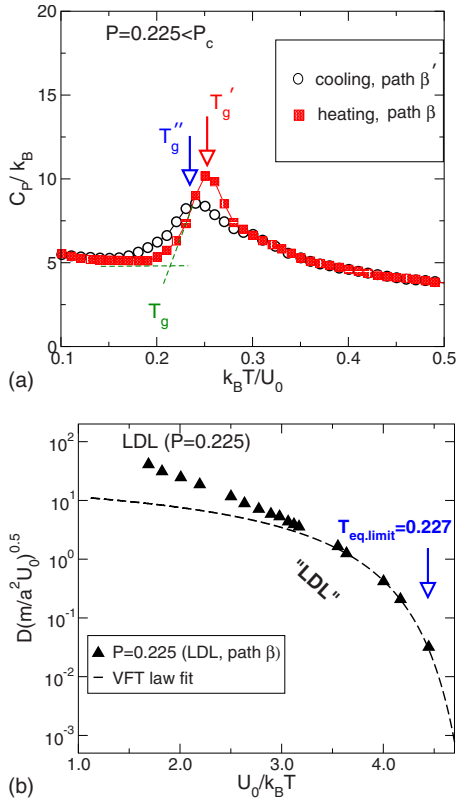

FIG. 3. (Color online) (a) Demonstration of nonergodicity by calculating the T dependence of C_P on cooling LDL along path β' for $P=0.225<P_c$. C_P increases and shows a maximum at $T_g''\approx 0.24$; further cooling results in a LDA glass. Upon heating LDA along path β, a sharp increase in C_P occurs as $T\to T_g$ and C_P displays a maximum at $T_g'\approx 0.26$. The standard construction (denoted by the dashed straight lines) indicates that, at the present pressure, the GT temperature is $T_g\approx 0.22$. We use a fast cooling or heating rate $q_2=2\times 10^{-6}q_0$ to avoid crystallization. (b) Demonstration of the agreement of the GT temperature T_g obtained from C_P calculations with the GT obtained from diffusivity measurements of the equilibrium liquid. The dashed line is a Vogel–Fulcher–Tamann fit. The lowest temperature where LDL can be obtained in equilibrium conditions is $T_{\text{eq.limit}}\approx 0.227$. This value is in agreement with the value $T_g\approx 0.22$ obtained from C_P.

The high-density liquid (HDL) is expected to transform into a HDA solid upon isobaric cooling at $P>P_c$ [path α' in Fig. 1(b)]. Similarly, the low-density liquid (LDL) should transform into a low-density amorphous (LDA) solid upon cooling at $P<P_c$ [path β' in Fig. 1(b)]. However, the vitrification of monatomic liquid cannot be assumed even in simulations[8,50] since crystallization will usually occur during the cooling process.

We find that HDA can indeed be formed if the liquid is cooled at a "slow" rate $q_1=1\times 10^{-6}q_0$ at $P>P_c$ (path α'). However, cooling the liquid at $P<P_c$ (path β') at the same rate results in crystallization. A faster ("intermediate") rate, $q_2=2\times 10^{-6}q_0$, is required in order to obtain LDA. We note that upon cooling along path β', the liquid with LDL-like local geometry crosses the LLPT coexistence line [Fig. 1(b)]. However, the LDL-to-HDL spinodal is never crossed so the system remains in the LDL phase due to metastability. Therefore, further cooling leads to vitrification of solid LDA without HDL formation.

Upon cooling the liquid at $P>P_c$ (path α'), although the system is in the one-phase region, a smooth crossover (*not* a transition) occurs from more LDL-like local geometry at temperatures well above the Widom line $T>T_W$ to more HDL-like local geometry well below the Widom line[26] [Fig. 1(b)]. The structural heterogeneities that characterize the Jagla liquid[51] are such that for $T<T_W$ the system can be thought of as a sea of molecules with locally LDL-like geometry, in which isolated molecules (and small clusters of molecules) with locally HDL-like geometry appear. As T decreases, the clusters of molecules with locally HDL-like geometry increase in number and size until there is a crossover at T_W. For $T<T_W$, the system can be thought of as a sea of molecules with locally HDL-like geometry, in which only isolated molecules (and small clusters of molecules) with locally LDL-like geometry occur. Thus one observes vitrification of the liquid with HDL-like local geometry to HDA.

Figure 2 compares the radial distribution functions (RDFs) of LDA and HDA obtained along $P=0.225<P_c$ and $P=0.275>P_c$, respectively. Both RDFs are clearly different indicating that LDA and HDA are indeed distinct glass phases. For LDA, the majority of the particles are located around the soft-core distance, in the vicinity of the minimum of the pair potential (corresponding to the peak of the RDF at the soft-core distance $r/a=1.72$ in Fig. 2). For HDA, neighbors are observed at both the hard-core distance ($r/a=1$) and the soft-core distance.

B. Relation between the glass transition and the liquid-liquid phase transition

A common experimental technique for studying the GT is DSC, which detects the GT by a maximum in C_P upon heating the glass back to the liquid state. A maximum in C_P also occurs in systems with LLPT. The corresponding maxima, obtained at different pressures in the supercritical region, form a line that, as the LLCP is approached, becomes the Widom line (the locus of maximum correlation length).[26] Some systems, such as the Jagla model, present both the GT and LLPT. Here we ask (i) how the GT and LLPT would be detected in DSC experiments and (ii) if the GT and LLPT are related.

Figure 3(a) shows C_P, both upon cooling LDL to LDA along path β' at $P=0.225<P_c$ and upon heating LDA along path β (back to LDL). Here, path β' does not cross the LDL spinodal [Fig. 1(b)]. Upon cooling, C_P increases while in LDL but starts to decrease as the system goes through the GT. On reheating we see the same relaxational overshoot of C_P as in typical GT experiments. Therefore, for path β' ($P<P_c$), where no Widom line is crossed and hence no signature of a LLPT in C_P is present, we find the standard GT phenomenology of glasses (including metallic glasses).

Note also from Fig. 3(a) that the GT "peak"—i.e., the overshoot observed in C_P upon heating—occurs at $T_g' \approx 0.26$, higher than the first point of decrease in C_P seen during cooling, which we denote T_g''. A standard construction based on the shape of the peak of C_P (Refs. 35 and 44) results in a GT temperature $T_g \approx 0.22$, where T_g is defined as the intersection of two linear fittings to C_P below and above the GT [Fig. 3(a)]. This T_g is the temperature that coincides, for laboratory glasses, with the fictive temperature[44] and also with the midpoint of the cooling transition.[52]

We note that the value $T_g \approx 0.22$ that we obtained from C_P, by a construction in the out-of-equilibrium domain of the cooling rate experiment, corresponds to the temperature of our lowest temperature diffusivity run, which was conducted on a fully equilibrated sample, by virtue of very long equilibration times. The diffusion constant for LDL at $P=0.225$ is shown in Fig. 3(b) for different temperatures. We include simulation results for only those state points where the system reaches equilibrium within the "time scales" accessible in computer simulations. The lowest temperature where LDL can be obtained in equilibrium conditions is $T_{\text{eq.limit}} \approx 0.227$, so $T_g \approx T_{\text{eq.limit}}$.

The phenomenology associated with the GT is more complicated at $P>P_c$ (path α'). Figure 4(a) shows C_P upon cooling the system at different $P>P_c$. We observe an increase in C_P as the Widom line temperature T_W is approached. The C_P maxima at T_W obtained at different pressures define the Widom line[26] [see Fig. 1(b)]. In the Jagla model, T_W occurs in the equilibrium regime.[26] The GT occurs at much lower temperature, at $T<T_W$. Upon further cooling below T_W, C_P starts to rapidly decrease and develops a shoulder but we find no GT peak. Upon heating the HDA glass at the same pressure back to the liquid phase, C_P shows two peaks [Fig. 4(b)]. The low-temperature peak at $T_g' \approx 0.3$ corresponds to the GT and is caused by the recovery of ergodicity upon heating. The high-temperature peak occurs in the equilibrium liquid phase at T_W, upon crossing the Widom line.[26] Thus, the behavior of C_P upon cooling and heating nearly coincides above T_g'.

Figure 4(b) shows for $P>P_c$ the same construction of Fig. 3(a) used to calculate T_g at $P<P_c$. We obtain $T_g \approx 0.27$. As found at $P<P_c$, this value is in agreement with diffusivity calculations. The lowest temperature where HDL can be obtained in equilibrium conditions (within the time scales accessible in computer simulations) is $T_{\text{eq.limit}} \approx 0.277$. Thus, the ergodicity limit in the present simulations is $T_{\text{eq.limit}} \approx T_g$.

We note that T_g is weakly P-dependent and it is continuous within either the LDL or HDL phases. However, T_g shows an apparent discontinuity upon crossing the LLPT line. This interesting result can be used in experiments to test whether a liquid presents polyamorphism. For example, in some substances such as water, crystallization occurs just

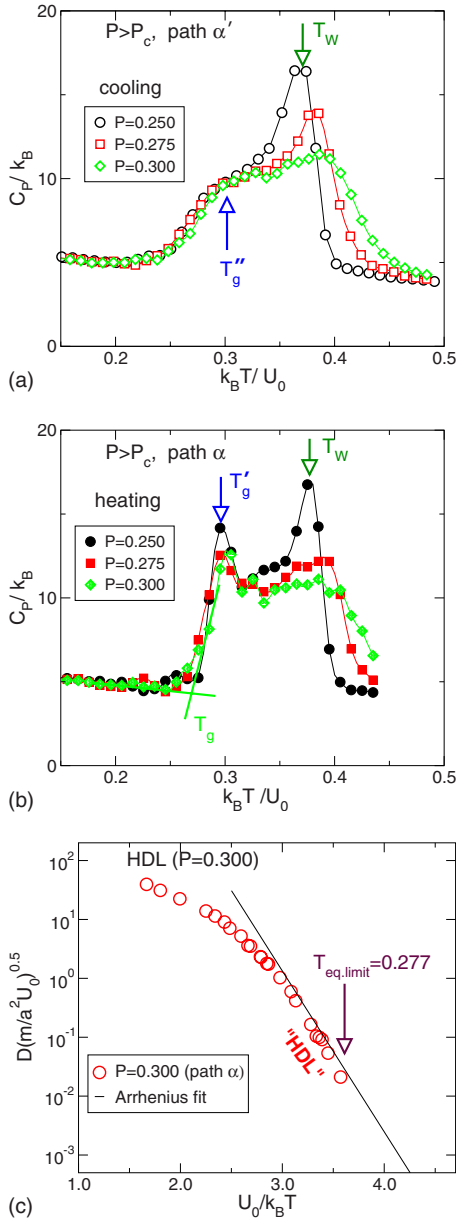

FIG. 4. (Color online) Contrast of C_P behavior near T_g and T_W and illustration of nonergodicity for the temperature dependence of the HDL specific heat C_P for $P>P_c$. (a) Cooling LDL along path α' and (b) heating along path α at different pressures $P>P_c$. Upon cooling, C_P shows a maximum at $T=T_W$ and a shoulder at $T_g'' \approx 0.3$, below which the liquid vitrifies to HDA. In contrast, upon heating HDA, C_P shows a peak at T_g', characterizing the GT and corresponding to the shoulder found upon cooling in (a). The standard construction as in Fig. 3 gives $T_g \approx 0.27$. Further heating results in a second peak at the Widom line, $T=T_W$. While T_g is nearly constant at $P>P_c$, the Widom line temperature T_W shifts to higher values as P increases. Moreover, due to critical fluctuations as $P \to P_c$, the height of the Widom line peak is much more sensitive to P than that corresponding to the GT. We use a slow cooling rate of $q_1=1\times10^{-6}q_0$, since crystallization is not observed for $P>P_c$. In summary, parts (a) and (b) demonstrate that the GT peak is not sensitive to P but is sensitive to heating vs cooling, while the Widom line peak is sensitive to P but not to heating vs cooling. (c) Diffusion coefficient as a function of temperature in the liquid phase. The lowest temperature of the equilibrium liquid accessible in simulations is $T_{\text{eq.limit}}=0.277$. This value is in agreement with the value $T_g=0.27$ obtained from C_P in (b).

above T_g. In this case, isothermal compression of LDL into HDL cannot be performed at $T \approx T_g$ since crystallization can occur. Thus, the presence of polyamorphism cannot be tested close to T_g by compression of LDL. In this cases, measuring T_g at different pressures and identifying a discontinuity would indicate that polyamorphism in the glass state extends above T_g to the liquid phase.[53]

Figure 4 also shows that C_P is weakly dependent on P near T_g. This means that practically the same enthalpy relaxation occurs across T_g for different P and that such a relaxation is not affected by the presence of the LLPT. Instead, C_P is P-dependent across the Widom line. In particular, it is notable that as $P \to P_c$, more and more of the liquid C_P is subsumed into the Widom peak. Thus, DSC can distinguish the GT from the Widom line associated with the LLPT.

The phenomenology associated with the GT is apparently the same for both LDL and HDL. The only difference is that, at $P > P_c$, the Widom line results in additional enthalpy changes (reflected in the C_P peak) not present at $P < P_c$. These additional enthalpy changes apparently add to, but do not interfere with, the enthalpy changes associated with the GT. To show this we calculate C_P upon cooling HDL at $P=0.4$, far above the critical pressure, so critical fluctuations should play a weak role, not interfering with the glass transition. Figure 5(a) shows C_P on cooling HDL at $P=0.4$ and LDL at $P=0.225$. At $P=0.4$, the Widom line peak in C_P is barely visible. For both LDL and HDL cooling, we observe a similar GT peak just above the corresponding T_g values. We also include, in Fig. 5(a), C_P obtained upon cooling HDL at $P=0.225$. At this pressure HDL is metastable relative to LDL [see Fig. 1(b)]. We observe that both cooling paths for HDL, at $P=0.225$ and at $P=0.4$, result in the same value of T_g and a similar behavior of C_P—at least for $T<0.3$. From Fig. 5(a) we see that the HDL phase at $P=0.225$ has a much higher C_P than the LDL phase at $P=0.225$ and the HDL phase at $P=0.4$. This larger value of C_P at $T \approx 0.3$ and $P=0.225$ is probably because, at these conditions, HDL is very close to the HDL-to-LDL spinodal [see Fig. 1(b)].

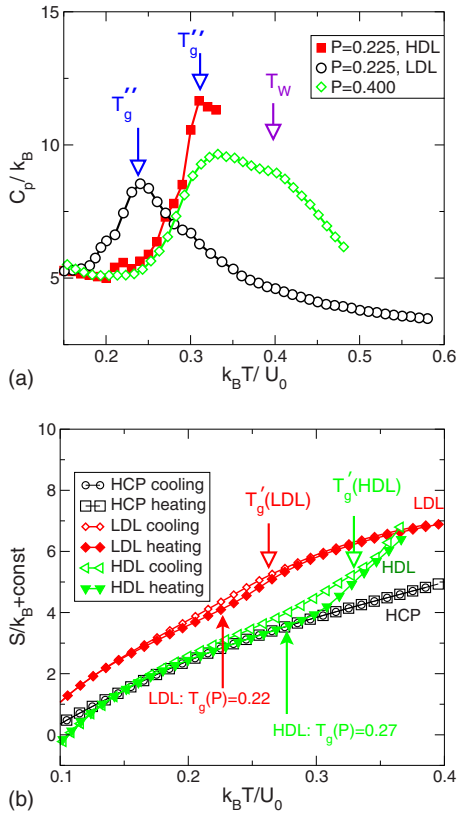

FIG. 5. (Color online) (a) Demonstration that when the effects of the Widom line are suppressed, the GT behavior of C_P is similar for the two phases LDL and HDL. Comparison of the constant-pressure specific heat C_P upon cooling both liquid phases, LDL and HDL. The HDL specific heat is shown for both high ($P > P_c$) and low ($P < P_c$; metastable relative to LDL) pressures. At high pressures, the Widom line peak is barely noticeable and the resulting C_P upon cooling HDL at $P=0.4$ [path α' of Fig. 1(b)] is similar to the C_P obtained upon cooling LDL at $P=0.225$ (path β'). The same GT phenomenology is observed above and below the critical pressure P_c if the Widom line effects at $P > P_c$ are suppressed. Cooling HDL at $P=0.225$ (solid squares) results in the same T_g as that obtained by cooling at $P=0.4$. However, since the $P=0.225$ path approaches the HDL spinodal [Fig. 1(b)], C_P is larger at $T \approx 0.3 > T_g$ for $P=0.225$ (path β') than for $P=0.4$ (path α'). (b) The dependence of the total entropy (without the kinetic contribution, $\frac{3}{2}k_B \ln T$) on temperature at constant pressure $P=0.22 < P_c$ for the hcp crystal and both types of amorphous states, HDL/HDA and LDL/LDA. The difference between the entropies of HDL and LDL, $S_{\mathrm{LDL}} - S_{\mathrm{HDL}} = 1.32k_B$ at $T=0.32$, is computed by thermodynamic integration around the critical temperature along the path $[P=0.22, T=0.32] \to [P=0.22, T=0.4] \to [P=0.4, T=0.4] \to [P=0.4, T=0.32] \to [P=0.22, T=0.32]$. The entropy difference between LDL and hcp is $\Delta S = \Delta H / T_m = 2.1k_B$, where $\Delta H = 0.73U_0$ is the enthalpy of fusion and $T_m = 0.345$ is the equilibrium melting temperature of the hcp crystal into LDL at $P=0.22$. The entropy undetermined constant is the same for hcp, LDL, and HDL. The difference between the entropies of HDA and LDA upon cooling and heating is caused by the ergodicity break at the glass transition. In all cases the heating/cooling rate is q_2.

C. Entropies of the two liquid phases

Next, we consider the entropies of the two liquid phases as they interconvert and as they vitrify. We find different entropies for the HDL and LDL phases as the temperature falls below the critical temperature. The differences can be assessed from the heat capacities seen in Fig. 5(a). We find that above the GT, the constant-pressure specific heat of the HDL phase is always greater than that of the LDL phase. Figure 5(a) shows C_P along path α' (cooling) for HDL at $P=0.4 \gg P_c$, where the Widom peak becomes very broad and shallow and the main peak is clearly related to the GT at $T=T_g'' \approx 0.33$. At $P=0.225 < P_c$, we calculate C_P of HDL only below the spinodal temperature $T=0.35$ at which HDL loses its stability and spontaneously transforms into LDL. Near the spinodal, K_T and C_P diverge, and this divergence contributes to a larger peak at $T_g'' \approx 0.31$. The HDL phase is thus losing entropy at a greater rate than the LDL phase. Hence it is not surprising to find that the HDL phase breaks ergodicity and becomes a glass at a higher temperature. The two glass temperatures T_g indicated in Fig. 5(a) are the temperatures taken from Figs. 3 and 4. They are seen to lie close to the temperature at which the two liquids start to fall out of equilibrium during the cooling process, indicated by the abrupt falloff in C_P.

To add quantitative detail to this scenario, we calculate the total entropies of the two liquid phases (minus their kinetic entropies, $-\frac{3}{2}k_B \ln T$) and present them relative to the entropy of the crystal $\left(-\frac{3}{2}k_B \ln T\right)$ in Fig. 5(b). Note that it is not possible, in the case of the Jagla model, to follow the

previous practice of subtracting a crystal-like harmonic entropy from total entropy and thus to examine the behavior of the configurational part of the total entropy. In the Jagla model, the potential energy landscape does not have harmonic basins as for systems with finite-second-derivative interaction potentials. Hence particle motions in a jammed configuration remain gaslike, and there is no strict equivalent of a "vibrational manifold" (density of states).

Figure 5(b) shows interesting features which will be important to study in future work on models of the Jagla type with continuous potentials[54] in which the decomposition into vibrational and configurational components will be possible. The entropy of the LDL phase S_{LDL} at the temperature $T=0.33$ is larger than that of the HDL phase S_{HDL} by $1.32k_B$ (assessed by a thermodynamic cycle around the critical point), and remains larger at all lower temperatures because of the larger specific heat of the HDL phase. S_{HDL} rapidly approaches the entropy of the crystal phase but instead of passing below it, encounters the GT at T_g, and the rapid entropy decrease is arrested. The total entropy of HDL (now HDA) thus remains close to the crystal value at lower temperatures. However, because this crystal is of very low density (even lower than LDA) its gaslike entropy is much larger than that of HDA. Thus the entropy equality does not have the significance of an "ideal glass transition" as would otherwise be implied.[55] By contrast, the entropy of the LDL phase, whose gaslike entropy component should be comparable with that of the low-density crystal, remains well above that of the crystal as the liquid falls out of equilibrium at its lower T_g. Thus as far as can be deduced for the Jagla potential, entropy relations at T_g remain the familiar ones, i.e., the entropy of the glass remains larger than the entropy of the crystal.

D. Effect of heating rates on the glass transition

Next, we study the heating rate effects on C_P across the GT and Widom line. Figure 6(a) shows C_P upon heating LDA at slow ($q=q_1$), intermediate ($q=q_2=2q_1$), and fast ($q=q_3=4q_1$) rates. The plot of C_P for $q=q_2$ is taken from Fig. 3(a). We clearly observe that the heating rate has drastic effects upon heating LDA.

In particular, heating LDA above T_g at a slow rate $q=q_1$ results in crystallization. At this slow rate, the particles have sufficient time to form crystal nuclei. Thus, the system spontaneously crystallizes into the hcp crystal, which has a lower free energy than the metastable liquid. This crystallization is associated with the release, upon heating, of latent crystallization heat, which results in an apparent specific heat *minimum* [Fig. 6(a)]. Upon further heating, the crystal finally melts at the melting temperature $T_m=0.32$, indicated by a strong endothermic peak in C_P. No crystallization event is observed upon heating at faster rates [Fig. 6(a)]. The behavior of C_P shown in Fig. 6(a) at a slow heating rate $q=q_1$ (i.e., a GT peak followed shortly by a crystallization peak and then by a melting peak) is very similar to that observed in the DSC experiments of Ref. 36, obtained upon heating glassy water at atmospheric pressure. We note that, due to the onset of crystallization, the peak associated with the GT observed at $q=q_2$ and $q=q_3$ is barely observed at $q=q_1$.

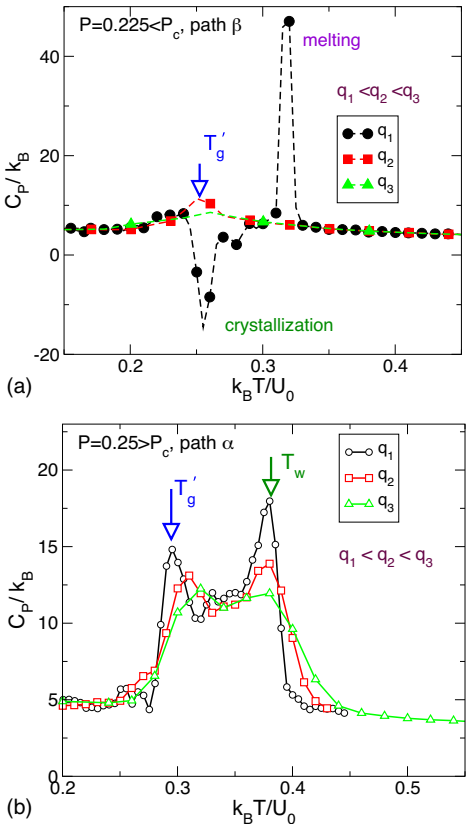

FIG. 6. (Color online) Effect of heating rate on the constant-pressure specific heat C_P. (a) Heating the glass along path β ($P<P_c$) at faster heating rates ($q=q_2$ and $q=q_3$) results in a liquid at $T>T_g'$. The GT temperature $T_g\approx 0.22$ (see Fig. 2) barely changes when using heating rates of $q=q_2$ or $q=q_3$. Heating the glass with a slow heating rate, $q=q_1$, results in a hcp crystal, which is of lower density than the LDA. The apparent specific heat minimum at $T\approx 0.25$ due to crystallization largely suppresses the GT peak observed with faster cooling rates at the same temperature. The hcp crystal melts upon further heating and produces an endothermic peak in C_P at $T\approx 0.32$. Note that the ratio of the GT temperature $T_g\approx 0.22$ and the melting temperature $T_m\approx 0.32$ is 2/3, thus mimicking the classical glassformers [the "2/3 value" due to Kauzmann (Ref. 55)]. (b) When heating the glass along path α ($P>P_c$), no crystallization occurs at the studied heating rates. As the heating rate increases, the GT peak at $T=T_g'$ shifts to higher temperature as expected. In contrast, the Widom line peak does not shift with heating rate.

The effect of heating rates along path α ($P>P_c$) is illustrated in Fig. 6(b). Both the GT peak at $T=T_g'$ and the Widom line peak at $T=T_W$ become less pronounced as the heating rate increases, but only the GT peak shifts in temperature for different q. These effects of the heating rate on the GT peak are qualitatively consistent with the experimental results.[1] The Widom line peak (at $T=T_W$) in principle should not depend on the heating rate. However, along $P=0.25$, which is very close to P_c, the magnitude of the Widom line peak decreases for fast heating rates. This is due to the critical slowing down of dynamics near the LLCP. Nevertheless, the position of the peak at T_W and the total area under the curve (enthalpy change) do not change with heating rate.

E. Thermal expansion

In addition to the constant-pressure specific heat, we study the thermal expansion coefficient,

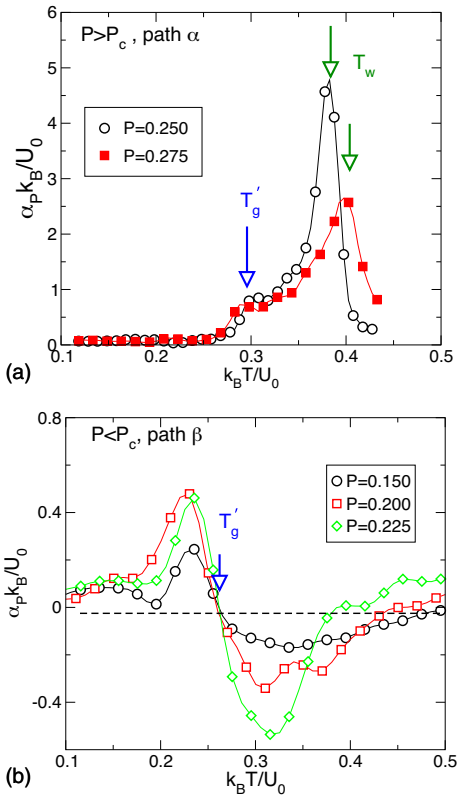

FIG. 7. (Color online) Thermal expansion coefficient α_P as a function of T. (a) Upon heating the glass along path α no density anomaly occurs (i.e., $\alpha_P > 0$). Note that α_P shows a large peak at the Widom line temperature T_W and a small shoulder at T_g'. (b) Upon heating along path β, $\alpha_P > 0$ and develops a peak at the GT temperature, $T_g \approx 0.22$ (see Fig. 3). Upon further heating, α_P becomes negative for a range of temperatures, implying that the liquid experiences a density anomaly (i.e., it expands upon cooling). The density anomaly region is confined by the temperature of minimum density ($T_{\min}$) and temperature of maximum density ($T_{\max}$) (see also Fig. 9). We note that $T_{\min} \approx T_g'$, i.e., the GT peak temperature defined in Fig. 3(a). Heating rates in panels (a) and (b) are $q_1 \equiv 1 \times 10^{-6} q_0$ and $q_2 \equiv 2 \times 10^{-6} q_0$, respectively.

$$\alpha_P \equiv \frac{1}{V}\left(\frac{\partial V}{\partial T}\right)_P, \tag{1}$$

which measures the change in volume as a response to the change in temperature at constant P. Figure 7 shows α_P upon heating the system at pressures above and below P_c.

Upon heating HDA along path α ($P > P_c$) from $T=0.1$ [Fig. 7(a)], the behavior of α_P suggests two transitions: one is the GT, indicated by a weak peak at $T_g' \approx 0.30$, and the second transition is associated with the LLPT, indicated by a larger peak at the Widom temperature $T_W \approx 0.4$.

In contrast, upon heating LDA along path β ($P < P_c$), α_P shows a very different behavior: a positive peak (maximum) at the GT, followed by negative peak (minimum) at higher temperature [Fig. 7(b)]. According to Eq. (1), when $\alpha_P < 0$, the volume of the system shrinks as the temperature increases. Thus a negative α_P is an indication of the density anomaly. For each pressure, the temperatures at which $\alpha_P = 0$ correspond (a) to the temperature of maxima density ($T_{\max}$) and (b) to the temperature of minimum density ($T_{\min}$). Here $T_{\min}$ approximately coincides with T_g' at relatively high pressures below the LDL spinodal. [Fig. 7(b)]. We will discuss $T_{\min}$ in detail in Sec. III F.

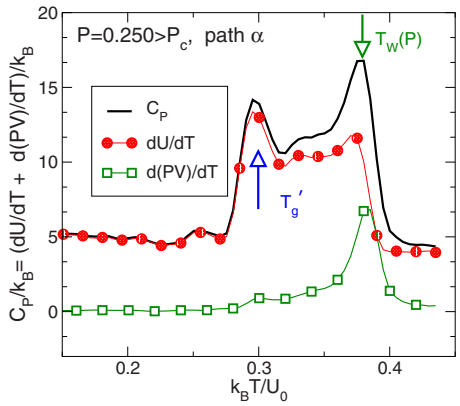

FIG. 8. (Color online) Contributions to the constant-pressure specific heat from the internal energy $(\partial U/\partial T)_P$ and the volume $P(\partial V/\partial T)_P$. The energy term contributes to C_P at both the GT and Widom line peaks. Instead, the volume term contributes only to the Widom line peak since the Widom line is associated with a LLCP and, thus, with density fluctuations. Instead, the GT represents the loss of molecular motion; fluctuations in volume are thus suppressed, so the bottom curve has a peak at T_W but not at T_g'.

We next discuss the sources of the two exothermic peaks of C_P at $P > P_c$ (see Fig. 8). The constant-pressure specific heat can be decomposed into two parts:

$$C_P \equiv \left(\frac{\partial H}{\partial T}\right)_P = \left(\frac{\partial (U+PV)}{\partial T}\right)_P = \left(\frac{\partial U}{\partial T}\right)_P + P\left(\frac{\partial V}{\partial T}\right)_P, \tag{2}$$

where H and U are the enthalpy and the internal energy. The first and second terms on the right-hand side of Eq. (2) are the contributions from the internal energy and the volume of the system, respectively. At the GT, the change in $(\partial U/\partial T)_P$ is more pronounced than the change in $P(\partial V/\partial T)_P$, which is negligible below T_g'. Instead, at $T \approx T_W$ both terms in Eq. (2) are relevant. The small contributions of $P(\partial V/\partial T)_P$ at $T \approx T_g'$ are due to the suppression of diffusivity across the GT, resulting in a small volume change. Instead, large volume fluctuations can be expected at $T \approx T_W$ since the Widom line arises as a consequence of the LLCP. Accordingly, there are large contributions of $P(\partial V/\partial T)_P = PV\alpha_P$ at $T \approx T_W$.

F. Density maximum and density minimum

The display of a temperature of maximum density is the first requirement of a model with claims to display waterlike character. It is a striking feature of the Jagla model, as described earlier[26] and is displayed in Fig. 9. What is remarkable, and not reported before, is the existence of the even rarer density minimum. This feature has been seen before only in supercooled Te, stable As_2Te_3 (Ref. 56) and some Ge–Te alloys,[57] and at the upper limit of experiments for BeF_2 (Ref. 58), in the simulations of water,[59,60] and a repulsive ramp model.[45] Very recently, the density minimum was observed in laboratory water in very low-temperature measurements, using noncrystallizing nanoconfined water[21] and silica.[61] In Fig. 9, the present simulations show how these features are unique to the low-density polymorph and vary in a complex way with pressure. The density maximum is always an equilibrium property, but the density minimum is only seen in the equilibrated liquid at the lowest pressures

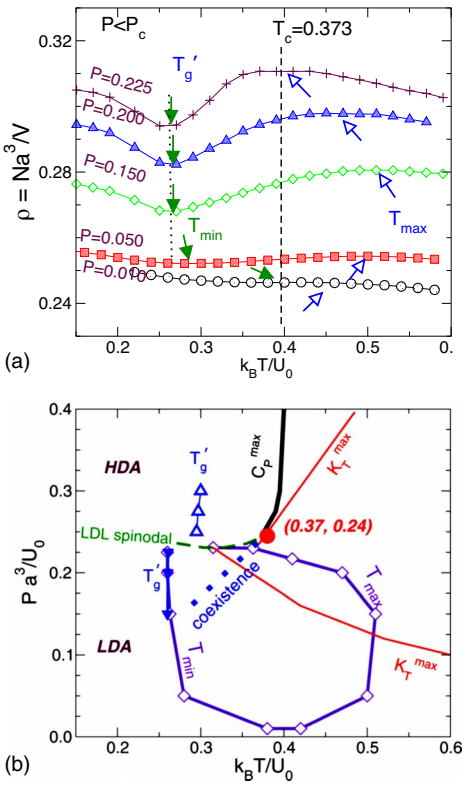

FIG. 9. (Color online) Demonstration of the effect of the GT on density minimum along path β for $P<P_c$. (a) For relatively high pressures below P_c ($0.05<P<P_c$), the density minima are located near T_g', along different β paths. For low pressures ($P<0.050$), the $T_{\min}$ is located in the ergodic region, and at $P\approx 0.01$, it approaches the temperature of maximum density ($T_{\max}$). The $T_{\max}$ line (open arrows) and the $T_{\min}$ line (filled arrows) confine the density anomaly region which disappears near the critical point and at very low pressure. (b) Density anomaly region is also shown in the P-T phase diagram. The LDL spinodal line is the boundary of density anomaly at higher pressures. The $T_{\max}$ line ends at the minimum of the LDL spinodal line. Both lines have zero slope at this point. The coexistence line extends into the one-phase region where the $C_P^{\max}$ line and the $K_T^{\max}$ line asymptotically merge into the Widom line region near the LLCP. The $K_T^{\max}$ line makes a loop on the P-T plane where it becomes $K_T^{\min}$ at high temperature (not shown), crosses the $T_{\max}$ line at the point of its maximum temperature, and ends at the LDL spinodal minimum.

($P<0.05$), in the temperature range between the T_g and the $T_{\max}$. At pressures between $P=0.1$ and the critical pressure P_c, the density minimum is pre-empted by the GT, for our cooling rates. For slower cooling rates the minimum would presumably continue to be seen as an equilibrium phenomenon. There is an apparent density minimum at T_g' due to the fact that the glassy state has a positive expansion coefficient.

Figure 9 emphasizes how the two extrema merge at low pressures and would also merge at higher pressures except for the phase change to HDA caused by intersection with the LDL spinodal.[62] According to the theorem proved in Ref. 62, the temperature of density maximum line meets the LDL spinodal at the point of its minimum on the P-T plane. Moreover, the slope of both curves at the point of their intersection must be equal to zero. Figure 9(b) is in complete agreement with these statements. No density anomaly is observed above the critical pressure upon crossing the Widom line. Therefore, the $T_{\min}$ and $T_{\max}$ are not caused by the Widom line in the Jagla model. The line of K_T maxima coincides with the Widom line near the critical point, but it forms a large loop in the P-T plane, crosses the $T_{\max}$ line at the point of its maximal temperature, and then turns upward to cross the $T_{\max}$ line at its ending point where they both meet the LDL spinodal. As we see above, this special point is a minimum of the LDL spinodal and maximum of the $T_{\max}$ line. It is also the common intersection of the LDL spinodal, the $T_{\max}$ line, and the compressibility maxima line.

The situation is quite different in the ST2 model of water,[60] in which the LLPT coexistence line and the Widom line have negative slopes. In this case the critical point lies in the region of the density anomaly and the $T_{\max}$ line enters the HDL region and meets the HDL spinodal at the point of its maximal pressure. The compressibility maximum line goes down from the critical point along the Widom line, crosses the $T_{\max}$ line at the point of its maximal temperature, makes a large loop on the P-T plane, encircles the critical point at high pressures, and crosses the $T_{\max}$ line at the HDL spinodal maximum. These examples show that the existence of $T_{\min}$ and $T_{\max}$ are always associated with the line of compressibility maxima which passes through the region of the density anomaly bounded by these two lines, but the Widom line does not necessarily lie in this region.

G. Pressure dependence of the glass transition

The normal behavior of the GT temperature is to increase with increasing pressure. It is found in the present system that this either does not occur (low-density phase) or occurs with barely detectable positive slope [Fig. 9(b)]. Here we show that such an anomaly is predictable from the anomalous behavior of the density, by invoking the second Davies–Jones relation of GT phenomenology.

The Davies–Jones relations are derivatives, for nonequilibrium transitions, of the Ehrenfest relations for second order phase transitions. For the case where $\Delta S=\Delta V=0$ on the coexistence line, Ehrenfest derived that[63]

$$dT/dP = VT\Delta\alpha/\Delta C_P. \tag{3}$$

For the case in which a process is arrested at a GT where the excess entropy S^{ex}=const (as postulated by Gibbs),[64] Davies and Jones derived the analogous relation[65]

$$dT_g/dP = V_g T_g \Delta\alpha/\Delta C_P, \tag{4}$$

where V_g is the volume at T_g and $\Delta\alpha$ and ΔC_P are the values measured at T_g. If we examine the change of α_P at the GT in the present system, we see (Fig. 7) that it is either very small (high-density phase) or weakly negative (low-density phase). In the latter case the complexity in the irreversible part of the transition zone must be ignored, as $\Delta\alpha$ in Eq. (4) is the difference between fully ergodic and fully frozen α values.

IV. SUMMARY AND DISCUSSION

In this work we have investigated the GT in the Jagla model, which was parametrized in order to show polyamorphism at high temperature, in the equilibrium liquid phase. This resulted in a unique system that has allowed us to study the relation between the GT and the LLPT. Below we discuss our findings and their implications to the understanding of

the glass state, which has been proposed as one of the most important open questions in contemporary science.[66]

We first have shown that the Jagla model provides an excellent example of a very simply constituted system that is a good glassformer and it is suitable for pursuing the study of glassforming ability, which is obviously a key issue in the science of bulk metallic glasses. Despite being monatomic, and also spherically symmetric in its interaction potential, this system proves vitrification during cooling at rates that are very moderate by simulation standards. The present results suggest that the presence of two scales in a pair interaction potential can be sufficient for a system to be a good glassformer. The ratio of these two length scales cannot be any value[49] since the present model, with different parametrizations, can crystallize extremely rapidly, indeed so rapidly that even computer quenching cannot avoid it.[31,67]

The Jagla model proves to have not only one but two very different liquids, which vitrify to different glasses upon cooling with rates common in computer simulations. These glasses are different amorphous forms both from the structural (e.g., their RDFs are distinct) and the thermodynamics point of view (e.g., their T_g values are different). In particular, we observed that T_g is practically constant for each glass but it is larger for HDA than for LDA. T_g shows an apparent discontinuity (of $\approx$17%) as we go from LDA to HDA across the transition line. The study of the relation between LDA and HDA and the possible transformations between each other are relevant to understand polyamorphism in the glassy state[12,13] and will be explored in a future work.[68]

The main goal of this work was to study how the GT phenomenology, as observed in the behavior of C_P upon cooling/heating, is affected in a system that has a LLPT. We found that for the two-scale Jagla model at $P < P_c$, where no Widom line is crossed, the glassforming behavior is similar to that observed in normal molecular and metallic glassformers. The same normal behavior is found also at $P \gg P_c$ so long as the pressure is maintained well separated from the LLCP pressure (so the LLCP fluctuations become irrelevant). It is only very close *above* to the LLCP that the long range cooperative fluctuations build up to dominate the behavior of C_P. Such LLCP fluctuations result in a second maximum in C_P, in addition to the first maximum associated with the GT. The corresponding maxima obtained at different pressures define the Widom line and occur at temperatures well above T_g for the present Jagla model parametrization.[26]

The presence of the Widom line results in a sharp increase in C_P upon cooling, as the Widom line temperature T_W is approached. Such a sharp increase in C_P is anomalous (i.e., in normal liquids, C_P decreases upon cooling) and is observed in few substances such as water.[69] It is therefore indeed reasonable to assert that the anomalous behavior of bulk water seen at normal and moderate pressures can be associated with the presence of a nearby LLCP and also to look for comparable behavior in other systems. However, it is then necessary to look comparatively at how the magnitude of the fluctuations (e.g., as quantified by the C_P maxima) are affected by proximity to the CP. It is obvious from Fig. 4 that, as the Widom line approaches the CP, the isobaric fluctuation effects on the response functions increase dramatically.

The effect of heating rates in the GT of LDA and HDA were also addressed. In particular, we found [Fig. 6(a)] that LDA is less stable against crystallization during reheating than is HDA; heating LDA or cooling LDL at a slow rate results in a hcp crystal. This is no doubt because LDA is closer in structure to the low-density crystal phase (hcp). The hcp structure is of density fractionally 8% smaller than that of LDA (like the relation between ice I_h and water). In this system, then, we have the unusual situation that HDL is less prone to crystallization than LDL. This makes an interesting contrast with most polyamorphic transitions that have been observed to date, in both laboratory experiments and simulations, in which the low-entropy phase (sometimes LDL, sometimes HDL) has always been found to crystallize more readily than the higher-entropy phase. This has suggested that the polyamorphic transition LDA to HDA, obtained upon isothermal compression of LDA,[4] is "merely" an Ostwald step on the route to the crystal state.[70] However, while this may be a common correlation, the behavior of the Jagla model establishes that it is not a necessary one.

A high-density crystalline phase has not been encountered in the present study. This is because the pressure range above 0.4 has not been investigated. Obviously, from Fig. 1(a), at high enough pressure this system will crystallize like any other hard sphere system. A potential analogous to the one investigated here but without the attractive ramp[45] spontaneously crystallizes into a rhombohedral structure at a density larger than the maximum density at which the density anomaly in the ρ-T plane is observed. A different hexagonal structure was found for this potential for even higher densities. It will be interesting to study which other crystalline phases[30] might exist at intermediate pressures, and how wide is the glassforming density range relative to that in the Stillinger–Weber siliconlike systems whose glassforming properties were investigated recently (see supplementary material in Refs. 8 and 50).

The Jagla model was originally proposed to model water's anomalous behavior[30] and an explanation for this has also been proposed.[49] We note here that the Jagla model, with different parameters from the ones used here, might be a good candidate to model cerium. Cerium crystallizes into hcp at low pressure, as the Jagla model does, and Ce–Al alloys show polyamorphism in the glass state.[10] It will be interesting to see if the Jagla model can be parametrized to yield other properties particular to cerium, such as its isosymmetric crystal-crystal (fcc-fcc) transition.[71] It is then understandable that the glass formation in cerium-based alloys is only obtained with multiple component doping, or very rapid quenching, as reported in the recent literature.[72]

Note added in proof. In 1970 the following observation was made about polyamorphism.[73] "the question raised here is whether it is proper to think in terms of vitreous polymorphs of a substance, i.e., whether long range disordered substances can generate sufficient differences in their short-range order, when prepared under different conditions, to have distinct and different thermodynamics properties, which

are maintained above their glass transition temperatures (when amorphous phase is in equilibrium) for a finite temperature interval." The present manuscript provides the definitive affirmative answer to this question, and also proves incorrect a second part of the same observation "For substances of small molecules such a situation could arise only when there is a high degree of directional character in the bonding...". Indeed, the present study confirms the view[24,26,30,49] that polyamorphism can arise from spherically symmetric interactions, so it is becoming increasingly plausible that the fundamental requirement for equilibrium polyamorphism is the presence of more than one distinct length scale in the interparticle interactions.

ACKNOWLEDGMENTS

We thank F. Mallamace, S. Sastry, and F. W. Starr for helpful discussions, I. Ehrenberg for important contributions at the earlier stage of this work, and NSF Grant No. CHE 0404673 for support. C.A.A. acknowledges support from NSF-DMR Grant No. 0454672. XML acknowledges support from World Premier International Research Center Initiative (WPI Initiative), MEXT, Japan. We also thank the Boston University Computation Center for allocation of CPU time. S.V.B. thanks the Office of the Academic Affairs of Yeshiva University for funding the Yeshiva University high-performance computer cluster and acknowledges the partial support of this research through the Dr. Bernard W. Gamson Computational Science Center at Yeshiva College.

[1] Recent reviews of supercooled and glassy water include P. G. Debenedetti, J. Phys.: Condens. Matter **15**, R1669 (2003); see also see also C. A. Angell, Science **319**, 582 (2008); P. G. Debenedetti and H. E. Stanley, Phys. Today **56**(6), 40 (2003); O. Mishima and H. E. Stanley, Nature (London) **396**, 329 (1998).
[2] E. F. Burton and W. T. Oliver, Nature (London) **135**, 505 (1935); Proc. R. Soc. London, Ser. A **153**, 166 (1935).
[3] C. G. Venkatesh, S. A. Rice, and A. H. Narten, Science **186**, 927 (1974).
[4] O. Mishima, L. D. Calvert, and E. Whalley, Nature (London) **314**, 76 (1985).
[5] O. Mishima, L. D. Calvert, and E. Whalley, Nature (London) **310**, 393 (1984).
[6] *New Kinds of Phase Transitions: Transformations in Disordered Substances*, *Proceedings of NATO Advanced Research Workshop*, edited by V. Brazhkin, S. V. Buldyrev, V. N. Ryzhov, and H. E. Stanley (Kluwer, Dordrecht, 2002).
[7] K. Katayama, T. Mizutani, K. Tsumi, O. Shinomura, and M. Yamakata, Nature (London) **403**, 170 (2000); G. Monaco, S. Falconi, W. A. Crichton, and M. Mezouar, Phys. Rev. Lett. **90**, 255701 (2003).
[8] H. Bhat, V. Molinero, V. Solomon, E. Soignard, S. Sastry, J. L. Yarger, and C. A. Angell, Nature (London) **448**, 787 (2007).
[9] R. Kurita and H. Tanaka, Science **306**, 845 (2004).
[10] H. W. Sheng, H. Z. Liu, Y. Q. Cheng, J. Wen, P. L. Lee, W. K. Luo, S. D. Shastri, and E. Ma, Nature Mater. **6**, 192 (2007).
[11] S. Sen, S. Gaudio, B. G. Aitken, and C. E. Lesher, Phys. Rev. Lett. **97**, 025504 (2006).
[12] M. C. Wilding, M. Wilson, and P. F. Mcmillan, Chem. Soc. Rev. **35**, 964 (2006).
[13] P. F. McMillan, J. Mater. Chem. **14**, 1506 (2004).
[14] C. A. Angell, Annu. Rev. Phys. Chem. **55**, 559 (2004).
[15] P. H. Poole, F. Sciortino, U. Essmann, and H. E. Stanley, Nature (London) **360**, 324 (1992).
[16] O. Mishima and H. E. Stanley, Nature (London) **392**, 164 (1998); O. Mishima, Phys. Rev. Lett. **85**, 334 (2000).
[17] J.-M. Zanotti, M.-C. Bellissent-Funel, and S.-H. Chen, Europhys. Lett. **71**, 91 (2005).
[18] Two recent reviews of experiments on quasi-two-dimensional and quasi-one-dimensional water are S.-H. Chen, F. Mallamace, L. Liu, D. Z. Liu, X.-Q. Chu, Y. Zhang, C. Kim, A. Faraone, C.-Y. Mou, E. Fratini, P. Baglioni, A. I. Kolesnikov, and V. Garcia-Sakai, AIP Conf. Proc. **982**, 39 (2008); H. E. Stanley, P. Kumar, G. Franzese, L. Xu, Z. Yan, M. G. Mazza, S.-H. Chen, F. Mallamace, and S. V. Buldyrev, AIP Conf. Proc. **982**, 251 (2008).
[19] L. Liu, S. -H.Chen, A. Faraone, C.-W. Yen, and C.-Y. Mou, Phys. Rev. Lett. **95**, 117802 (2005).
[20] S.-H. Chen, L. Liu, E. Fratini, P. Baglioni, A. Faraone, and E. Mamontov, Proc. Natl. Acad. Sci. U.S.A. **103**, 9012 (2006); S.-H. Chen, F. Mallamace, C.-Y. Mou, M. Broccio, C. Corsaro, A. Faraone, and L. Liu, *ibid.* **103**, 12974 (2006).
[21] The maximum in the coefficient of thermal expansion at the Widom line was recently reported in H_2O by F. Mallamace, C. Branca, M. Broccio, C. Corsaro, C.-Y. Mou, and S.-H. Chen, Proc. Natl. Acad. Sci. U.S.A. **104**, 18387 (2007); and in D_2O by D. Liu, Y. Zhang, C.-C. Chen, C.-Y. Mou, P. H. Poole, and S.-H. Chen, *ibid.* **104**, 9570 (2007).
[22] F. Mallamace, C. Corsaro, M. Broccio, C. Branca, N. Gonazalez-Segredo, J. Spooren, S.-H. Chen, and H. E. Stanley, Proc. Natl. Acad. Sci. U.S.A. **105**, 12725 (2008).
[23] S.-H. Chen, L. Liu, X. Chu, and Y. Zhang, J. Chem. Phys. **125**, 171103 (2006); P. Kumar, Z. Yan, L. Xu, M. G. Mazza, S. V. Buldyrev, S.-H. Chen, S. Sastry, and H. E. Stanley, Phys. Rev. Lett. **97**, 177802 (2006); F. Mallamace, S.-H. Chen, M. Broccio, C. Corsaro, V. Crupi, D. Majolino, and V. Venuti, P. Baglioni, E. Fratini, C. Vannucci, and H. E. Stanley, J. Chem. Phys. **127**, 045104 (2007); F. Mallamace, C. Branca, M. Broccio, C. Corsaro, N. Gonzalez-Segredo, H. E. Stanley, and S.-H. Chen, Eur. Phys. J.: Appl. Phys. **161**, 19 (2008).
[24] G. Stell and P. C. Hemmer, J. Chem. Phys. **56**, 4274 (1972); M. R. Sadr-Lahijany, A. Scala, S. V. Buldyrev, and H. E. Stanley, Phys. Rev. Lett. **81**, 4895 (1998); Phys. Rev. E **60**, 6714 (1999); A. Scala, M. R. Sadr-Lahijany, N. Giovambattista, S. V. Buldyrev, and H. E. Stanley, *ibid.* **63**, 041202 (2001); J. Stat. Phys. **100**, 97 (2000).
[25] G. Franzese, G. Malescio, A. Skibinsky, S. V. Buldyrev, and H. E. Stanley, Nature (London) **409**, 692 (2001); G. Malescio, G. Franzese, G. Pellicane, A. Skibinsky, S. V. Buldyrev, and H. E. Stanley, J. Phys.: Condens. Matter **14**, 2193 (2002); G. Franzese, G. Malescio, A. Skibinsky, S. V. Buldyrev, and H. E. Stanley, Phys. Rev. E **66**, 051206 (2002); A. Skibinsky, S. V. Buldyrev, G. Franzese, G. Malescio, and H. E. Stanley, *ibid.* **69**, 061206 (2004); G. Malescio, G. Franzese, A. Skibinsky, S. V. Buldyrev, and H. E. Stanley, *ibid.* **71**, 061504 (2005); G. Malescio, S. V. Buldyrev, and H. E. Stanley (unpublished).
[26] L. Xu, P. Kumar, S. V. Buldyrev, S.-H. Chen, P. H. Poole, F. Sciortino, and H. E. Stanley, Proc. Natl. Acad. Sci. U.S.A. **102**, 16558 (2005); L. Xu, S. V. Buldyrev, C. A. Angell, and H. E. Stanley, Phys. Rev. E **74**, 031108 (2006); L. Xu, I. Ehrenberg, S. V. Buldyrev, and H. E. Stanley, J. Phys.: Condens. Matter **18**, S2239 (2006).
[27] S. Sastry and C. A. Angell, Nature Mater. **2**, 739 (2003).
[28] T. Morishita, Phys. Rev. Lett. **87**, 105701 (2001).
[29] I. Saika-Voivod, P. H. Poole, and F. Sciortino, Philos. Mag. **412**, 514 (2001); Phys. Rev. E **63**, 011202 (2000); Nature **84**, 1437 (2004); I. Saika-Voivod, F. Sciortino, and T. Grande, Phys. Rev. E **70**, 061507 (2004).
[30] E. A. Jagla, J. Chem. Phys. **111**, 8980 (1999); J. Phys.: Condens. Matter **11**, 10251 (1999); Phys. Rev. E **63**, 061509 (2001); S. V. Buldyrev, G. Franzese, N. Giovambattista, G. Malescio, M. R. Sadr-Lahijany, A. Scala, A. Skibinsky, and H. E. Stanley, Physica A **304**, 23 (2002).
[31] H. M. Gibson and N. B. Wilding, Phys. Rev. E **73**, 061507 (2006).
[32] S. V. Buldyrev, P. Kumar, P. G. Debendetti, P. Rossky, and H. E. Stanley, Proc. Natl. Acad. Sci. U.S.A. **104**, 20177 (2007).
[33] E. Lomba, N. G. Almarza, C. Martin, and C. McBride, J. Chem. Phys. **126**, 244510 (2007).
[34] I. Kohl, L. Bachmann, E. Mayer, A. Hallbrucker, and T. Loerting, Nature (London) **435**, E1 (2005).
[35] N. Giovambattista, C. A. Angell, F. Sciortino, and H. E. Stanley, Phys. Rev. Lett. **93**, 047801 (2004); Phys. Rev. E **72**, 011203 (2005).
[36] G. P. Johari, A. Hallbrucker, and E. Mayer, Nature (London) **330**, 552 (1987).
[37] A. Hallbrucker, E. Mayer, and G. P. Johari, J. Phys. Chem. **93**, 4986 (1989).
[38] V. Velikov, S. Borick, and C. A. Angell, Science **294**, 2335 (2001).
[39] Y. Z. Yue and C. A. Angell, Nature (London) **427**, 717 (2004).
[40] Y. Z. Yue and C. A. Angell, Nature (London) **435**, E1 (2005).
[41] I. Kohl, L. Bachmann, A. Hallbrucker, E. Mayer, and T. Loerting, Phys.

Chem. Chem. Phys. **7**, 3210 (2005).
[42] C. A. Angell, J. Phys.: Condens. Matter **19**, 205112 (2007).
[43] M. S. Elsaesser, I. Kohl, E. Mayer, and T. Loerting, J. Phys. Chem. B **111**, 8038 (2007).
[44] C. T. Moynihan, P. B. Macedo, C. J. Montrose, P. K. Gupta, M. A. Debolt, J. F. Dill, B. E. Dom, P. W. Drake, A. J. Easteal, P. B. Elterman, R. P. Moeller, H. Sasabe, and J. A. Wilder, Ann. N. Y. Acad. Sci. **279**, 15 (1976).
[45] P. Kumar, S. V. Buldyrev, F. Sciortino, E. Zaccarelli, and H. E. Stanley, Phys. Rev. E **72**, 021501 (2005).
[46] D. C. Rapaport, *The Art of Molecular Dynamics Simulation* (Cambridge University Press, Cambridge, 1995).
[47] S. V. Buldyrev and H. E. Stanley, Physica A **330**, 124 (2003).
[48] S. V. Buldyrev, in *Aspects of Physical Biology*, Lecture Notes in Physics, edited by G. Franzese and M. Rubi (Springer-Verlag, Berlin, 2008), p. 97.
[49] Z. Yan, S. V. Buldyrev, N. Giovambattista, and H. E. Stanley, Phys. Rev. Lett. **95**, 130604 (2005); Z. Yan, S. V. Buldyrev, N. Giovambattista, P. G. Debenedetti, and H. E. Stanley, *ibid.* **73**, 051204 (2006); Z. Yan, S. V. Buldyrev, P. Kumar, N. Giovambattista, P. G. Debenedetti, and H. E. Stanley, *ibid.* **76**, 051201 (2007); Z. Yan, S. V. Buldyrev, and H. E. Stanley, *ibid.* **78**, 051201 (2008).
[50] V. Molinero, S. Sastry, and C. A. Angell, Phys. Rev. Lett. **97**, 075701 (2006).
[51] M. Canpolat, F. W. Starr, M. R. Sadr-Lahijany, A. Scala, O. Mishima, S. Havlin, and H. E. Stanley, Chem. Phys. Lett. **294**, 9 (1998); N. Giovambattista, S. V. Buldyrev, F. W. Starr, and H. E. Stanley, Phys. Rev. Lett. **90**, 085506 (2003); N. Giovambattista, M. G. Mazza, S. V. Buldyrev, F. W. Starr, and H. E. Stanley, J. Phys. Chem. B **108**, 6655 (2004); M. G. Mazza, N. Giovambattista, F. W. Starr, and H. E. Stanley, Phys. Rev. Lett. **96**, 057803 (2006); M. G. Mazza, N. Giovambattista, H. E. Stanley, and F. W. Starr, Phys. Rev. E **76**, 031203 (2007).
[52] C. A. Angell, Chem. Rev. (Washinton, D.C.) **102**, 2627 (2002).
[53] T. Loerting and N. Giovambattista, J. Phys.: Condens. Matter **18**, R919 (2006).
[54] P. A. Netz, S. V. Buldyrev, M. C. Barbosa, and H. E. Stanley, Phys. Rev. E **73**, 061504 (2006).
[55] W. Kauzmann, Chem. Rev. (Washinton, D.C.) **43**, 219 (1948).
[56] L. S. Tver'yanovich, V. M. Ushakov, and A. Tverjanovich, J. Non-Cryst. Solids **197**, 235 (1996).
[57] Y. Tsuchiya, J. Non-Cryst. Solids **60**, 960 (1999).
[58] M. Hemmati, C. T. Moynihan, and C. A. Angell, J. Chem. Phys. **115**, 6663 (2001).
[59] D. Paschek, Phys. Rev. Lett. **94**, 217802 (2005).
[60] P. H. Poole, I. Saika-Voivod, and F. Sciortino, J. Phys.: Condens. Matter **17**, L431 (2005).
[61] S. Sen, R. L. Andrus, D. E. Baker, and M. T. Murtagh, Phys. Rev. Lett. **93**, 125902 (2004).
[62] S. Sastry, P. Debenedetti, F. Sciortino, and H. E. Stanley, Phys. Rev. E **53**, 6144 (1996).
[63] P. Ehrenfest, Proc. Amsterdam Acad. **36**, 153 (1933).
[64] G. Adam and J. H. Gibbs, J. Chem. Phys. **43**, 139 (1965).
[65] R. O. Davies and G. O. Jones, Adv. Phys. **2**, 370 (1953).
[66] D. Kennedy and C. Norman, special issue of Science **309**, 75 (2005).
[67] J. Luo, L. Xu, S. V. Buldyrev, and H. E. Stanley (unpublished).
[68] L. Xu, S. V. Buldyrev, C. A. Angell, P. G. Debenedetti, H. E. Stanley, and N. Giovambattista (unpublished).
[69] M. Oguni and C. A. Angell, J. Chem. Phys. **78**, 7334 (1983).
[70] W. Ostwald, Z. Phys. Chem. **22**, 289 (1897).
[71] I. L. Aptekar and Y. G. Ponyatovskii, Fiz. Met. Metalloved. **25**, 777 (1968).
[72] B. Zhang, R. J. Wang, and W. H. Wang, Phys. Rev. B **72**, 104205 (2005).
[73] C. A. Angell and E. J. Sare, J. Chem. Phys. **52**, 1058 (1970): see footnote 39.